UNITED NATIONS EDUCATIONAL, SCIENTIFIC AND CULTURAL ORGANIZATION
INTERNATIONAL CENTRE FOR THEORETICAL PHYSICS
I.C.T.P., P.O. BOX 586, 34100 TRIESTE, ITALY, CABLE: CENTRATOM TRIESTE

H4.SMR/642 - 24

College on Methods and Experimental Techniques in Biophysics

28 September - 23 October 1992

Identification and Characterization of the Primary Donor in Bacterial Photosynthesis: a Chronological Account of an EPR/ENDOR Investigation

G. FEHER

University of California, U.S.A.

These are preliminary lecture notes, intended only for distribution to participants.

The Bruker Lecture

Identification and Characterization of the Primary Donor in Bacterial Photosynthesis: a Chronological Account of an EPR/ENDOR Investigation†

George Feher
University of California, San Diego, Department of Physics 0319, 9500 Gilman Drive, La Jolla, CA 92093-0319, USA

A chronological account is presented of the work that has led to the identification and characterization of the primary donor, D, in photosynthetic reaction centres (RCs) of *Rb. sphaeroides*. The observation that the EPR linewidth of D^+ is *ca.* 40% smaller than that of the bacteriochlorophyll ($BChl^+$) monomer *in vitro* led to the hypothesis that D^+ is a dimer in which the electron is shared between two bacteriochlorophylls. This was convincingly proved by ENDOR experiments that showed the spin densities in $BChl^+$ to be, on the average, twice as large as in D^+. The dimer model was confirmed a decade later, when the structure of the reaction centre (RC) was determined by X-ray diffraction. The electronic structure of D^+ was investigated by ENDOR both in solutions and in single crystals of RCs. The results showed that in the native dimer the spin density is asymmetrically distributed, favouring the A (also called the L) half by *ca.* 2:1. Electron densities were also obtained in two mutant RCs in which either one or the other BChl was changed to bacteriopheophytin (BPhe). The unpaired spin in these mutants (heterodimers) resides on the BChl half. The spin density distribution is significantly different in the two heterodimers and is also different from the spin density distribution in the respective halves of the homodimer. These differences point to the effect of the protein environment on the spin density. Molecular orbital calculations (RHF-INDO/SP) are in good agreement with the experimentally determined spin densities. The concluding section presents speculations on the possible advantages of a dimer over a monomer in the primary charge-separation process.

First let me thank you for having invited me to give the Bruker lecture. Having heard the names of past lecturers I feel delighted and honoured to be in their company. When Keith McLauchlan asked me for a title of the talk my first impulse was to reminisce about the old days of 40 years ago and to try to recapture the excitement and tribulations of all the problems that we worked on since. However, reminiscing smacks too much of old age so I decided instead to focus on one particular problem in which EPR played a key role, and on which we and other groups worked 'only' for the past ~25 years. But I can't pass up the opportunity to remark on the change in style of research involving EPR. Forty years ago there were no commercial instruments and a great deal of effort went into the design and building of the EPR spectrometer. This was followed by the search for a good problem. By contrast, we now have excellent commercial instruments (some manufacturers even sponsor talks like this) and EPR has become an accepted technique taking its rightful place among many others in the armory of scientific tools. Thus, there has been a transition in our lab, and I suspect in other labs as well, in the way we use EPR: from a 'Technique in Search of a Problem' to a tool to be kept in mind for solving specific problems.

The specific problem that I want to discuss deals with the identification and characterization of a free radical created in the primary process of photosynthesis. Although this project started over 20 years ago, it is still an active area of research. This paper is an attempt to lead the reader chronologically, through the various stages of development and thereby illustrating the evolution and progress that has been made. To set the stage a brief background on photosynthesis is given.

† Presented as the Bruker lecture at the 25th Annual International Conference of the ESR Group of the Royal Society of Chemistry, 'EPR of Organic and Biorganic Radicals,' held jointly with the Society of Free Radical Research at the University of York, 29th March to 2nd April 1992.

A Brief Overview of Photosynthesis

Green Plant vs. *Bacterial Photosynthesis.*—Photosynthesis is the biological process by which electromagnetic energy (light) is converted into chemical energy. Life on earth derives all its energy from this process. The first serious experiment in photosynthesis was performed about 200 years ago in the 1770s by Priestley, who did the following experiment. He took two bell jars and he put a mouse under each of them. He also put a plant under one of the bell jars but not under the other. The mouse with the plant lived much longer than the other mouse. From this experiment he correctly concluded that the plant, through the interaction with light, was modifying the air by producing some new substance. He set out to prove what this substance was and thereby discovered oxygen. Quite a spin-off from photosynthesis research—to discover a gas as important as oxygen. Very soon thereafter, he and others worked out the basic equation of green plant photosynthesis which is eqn. (1),

$$CO_2 + H_2O + h\nu \longrightarrow C(H_2O) + O_2\uparrow \qquad (1)$$

i.e., CO_2 plus H_2O in the presence of light, gives a carbohydrate—$C(H_2O)$. The reaction of green plant photosynthesis, as we know it today—as this equation stands today—is over 200 years old. So what have the researchers in photosynthesis been doing for 200 years? Where did the ten thousands of man-years of research go? Clearly though, this equation is misleadingly simple. It is just a net reaction covering the many events taking place in the complicated process of photosynthesis.

Before discussing what is known and what is not known, let us first take an overview of the whole field of photosynthesis. A

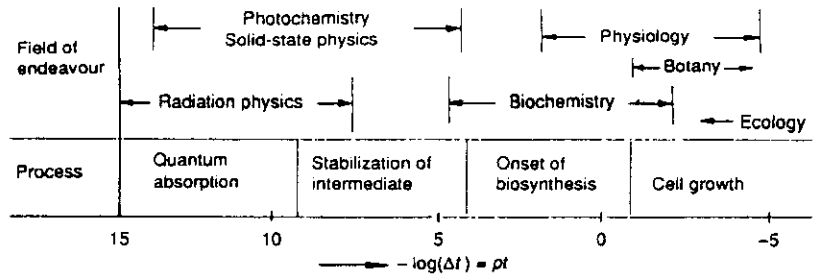

Fig. 1 'pt' diagram showing the various processes and fields of endeavour in photosynthesis. Δt is the time interval for a process to occur (modified from Kamen[1]).

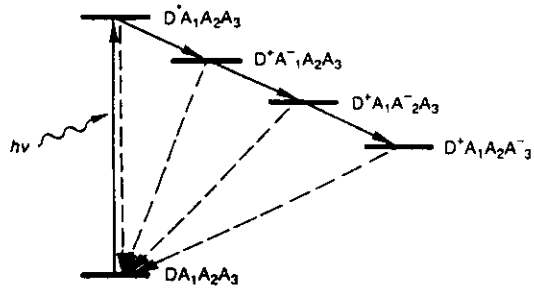

Fig. 2 Schematic representation of the initial charge-separation in bacterial photosynthesis. The absorption of a photon is followed by ejection of an electron from the excited donor D*. The electron is transferred to the acceptor A_1 and then shuttled through a series of acceptors A_2, A_3 ... The minimum unit capable of producing the charge separation is called the reaction centre (RC).

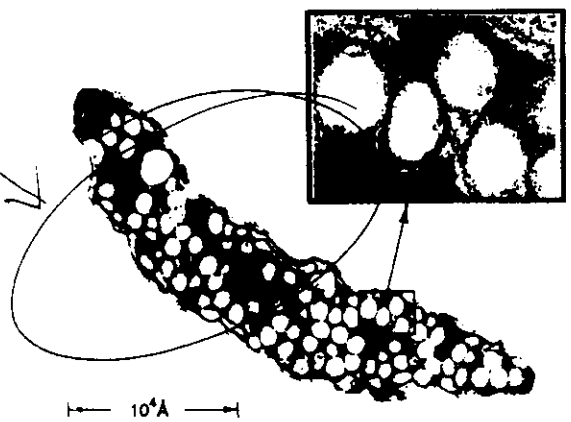

Fig. 3 Electron micrograph of a section of *Rh. sphaeroides* R-26. The round bodies represent invaginations of the plasma membrane. The RC is believed to span the membrane.

good way to do this is to represent the processes that occur in photosynthesis according to the time interval, Δt, that it takes for each process to occur. The time intervals can be as short as 10^{-15} s and as long as 10^7 s. 10^7 s is a year, the time it takes a tree to grow; 10^{-15} s is the time for the absorption of a photon. Because of the large range of times involved, it is convenient to plot the logarithm of the time interval, as shown in Fig. 1. One actually plots minus the logarithm of Δt, and in analogy with the hydrogen ion concentration, pH, this is called a 'pt' diagram. As far as I know, Kamen was the first one to present things in this way.[1] In Fig. 1 each pt value has a process and a field of endeavour associated with it. The processes start with a quantum absorption on the left, followed by stabilization of intermediates, onset of biosynthesis, and cell growth. The fields that are involved in photosynthesis cover a large range starting with radiation physics, followed by solid-state physics, and to the right, by ecology. So it's a truly interdisciplinary field. This, of course, causes problems because sometimes there is no common language between people working in greatly differing 'pt' ranges. So, if you meet somebody and he says he is working in photosynthesis, don't get too enthusiastic. Ask him, first, what his 'pt' range is—you may have nothing to talk about. When Martin Kamen first showed this slide (he gave a seminar in our physics department about 25 years ago), he had an additional ordinate labelled 'level of ignorance'. And that Level of Ignorance had a high peak around 'solid state physics', so that's how we got hooked—we thought maybe we could reduce the peak. I later heard that when Kamen gave the seminar to biochemists he had shifted the peak to 'biochemistry'. But it was too late—we were already involved. I am grateful to him for it, anyway.

What I would like to talk about is covered in the left part of the 'pt' diagram, called 'primary processes in photosynthesis.' 'Primary' here refers to the temporal events, *i.e.*, what happens at the beginning of the process when the photon impinges on the photosynthetic apparatus.

The system that we are working on is much simpler than green-plant photosynthesis, namely, bacterial photosynthesis. In green-plant photosynthesis, there are two systems, System I and System II. One system deals with the right-hand side of the photosynthesis equation, *i.e.*, oxygen evolution, while the other one deals with the left-hand side, *i.e.* CO_2 fixation. Bacteria are much simpler; they do not evolve oxygen, they have only one system. They have other advantages too. It is much easier to use the modern advances in molecular biology in bacteria than in green plants. Also, from a physics point of view, it is appealing to work with bacteria. After all, you take a few bacteria, you inoculate a bottle and in no time you have 10^8 bacteria cm^{-3}. It is essentially an ensemble of identical particles, a concept that physicists like to talk about. There was another very important reason why we entered the field. Bacterial photosynthesis was a very uncrowded field; very few people worked in it as compared with green-plant photosynthesis. Actually, I was surprised by this because it seemed logical that one would want to understand the simpler system before proceeding to a more complicated one. Kamen, being a wise man, knew the answer! 'Ah, that's because everybody is an m.c.p.'—m.c.p. standing for mammalian chauvinistic pig. Many people work on green plant photosynthesis just because we feed on spinach, or on animals that feed on spinach. But not being m.c.p.s, we went to work on the bacterial photosynthesis system. In particular, we focused on the early (primary) events of bacterial photosynthesis depicted in the left part of the 'pt' diagram.

The Primary Process of Bacterial Photosynthesis.—The primary process of bacterial photosynthesis is a charge separation, schematically illustrated in Fig. 2. Absorption of a

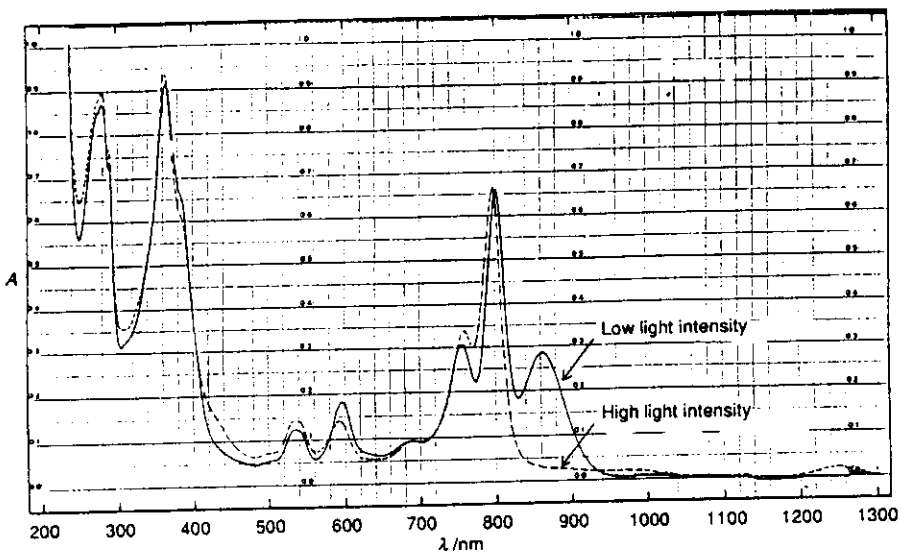

Fig. 4 Optical absorption spectrum of reaction centre from *Rb. sphaeroides* R-26 at T = 23 °C. Modified from ref. 4.

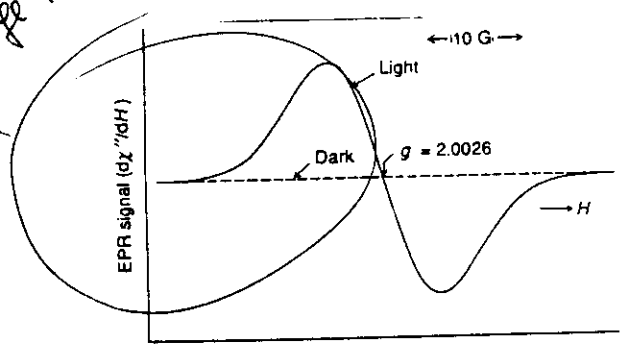

Fig. 5 Light-induced EPR signal from RCs of *Rb. sphaeroides* (ν_e = 9 GHz, T = 77 K)

photon excites the primary electron donor, a pigment molecule, from its ground state D to its excited state D*. This is followed by a transfer of an electron from D* to the acceptor A_1. The electron is subsequently shuttled through a series of acceptors, A_2, A_3 and the missing electron on D^+ is replaced by a secondary donor (not shown in Fig. 2). The remarkable feature of this electron-transfer chain is that the rate of the forward electron-transfer reaction (solid arrows) greatly exceeds the wasteful charge-recombination reaction (dashed arrows). Thus, the absorption of *one* photon results in the formation of *one* charge-separated pair, that is, the quantum yield of the process is close to unity—an achievement that remains unmatched in photochemical reactions in model systems.

How do EPR and ENDOR Enter into the Picture?—When we started to work in this field in the late sixties, the chemical identities of the primary reactants D_1, A_1, A_2, A_3 were not known. This seemed to us a scandalous affair. After two hundred years of research in photosynthesis, the identity of the basic actors remained a mystery!! But there was hope in the EPR camp: in each step of the electron transfer process one deals with species having an unpaired spin. Consequently, EPR held promise to be the technique of choice in trying to identify and characterize them. Furthermore, to understand and to be able to calculate the electron-transfer rates that give rise to the remarkable quantum yield of unity, one needs to know the detailed electronic structure of the charged species. ENDOR, which measures hyperfine couplings (hfs) and hence spin density and wavefunctions, provides the technique to address these questions. In this talk I do not want to describe the identification and characterization of all the reactants, but I will focus on one: the primary donor D. Before proceeding, I have to digress again and discuss the environment in which the reactants operate.

The Bacterial Reaction Centre (RC).—It was realized early on that it would be advantageous to isolate the smallest structural unit capable of producing the charge separation. This unit is called the reaction centre (RC), a term that was coined by Rod Clayton (RC!!) who did pioneering work in this field.[2] The existence of the RC had already been postulated in 1932 by Emerson and Arnold.[3] By 1970 a complex had been isolated from the photosynthetic bacterium *Rhodobacter* (*Rb*) *sphaeroides*[4,5] that continues to serve as a model RC to this day. It is an integral membrane protein, *i.e.*, it sits inside (spans) the plasma membrane of the bacterium (Fig. 3). It has a molecular weight of *ca.* 100 kDa and is composed of three subunits L, M and H and the following cofactors which are involved in the electron transfer process: four bacteriochlorophylls, two bacteriopheophytins, two quinones and one non-haem high-spin Fe^{2+} (for a review see ref. 6). Thus, the protein can be viewed as a scaffolding holding the electron transfer reactant in just the right juxtaposition to produce the high quantum yield.

Identification of the Primary Donor

Comparison of the Kinetics of the Optical Changes and the EPR Signal.—The optical spectrum of the purified RC is shown in Fig. 4. Let us focus on the near infrared peak at 865 nm. At low light intensities few RCs will be optically excited and the spectrum will be that of the ground state $DA_1A_2A_3$ (see Fig. 2). At high light intensities a significant fraction of RCs will be in one of the charge-separated states, say $D^+A_1A_2A_3^-$. The reduction (bleaching) of the 865 nm peak that occurs at high light intensity signifies that one of the electron transfer reactants is responsible for this absorption. This phenomenon was

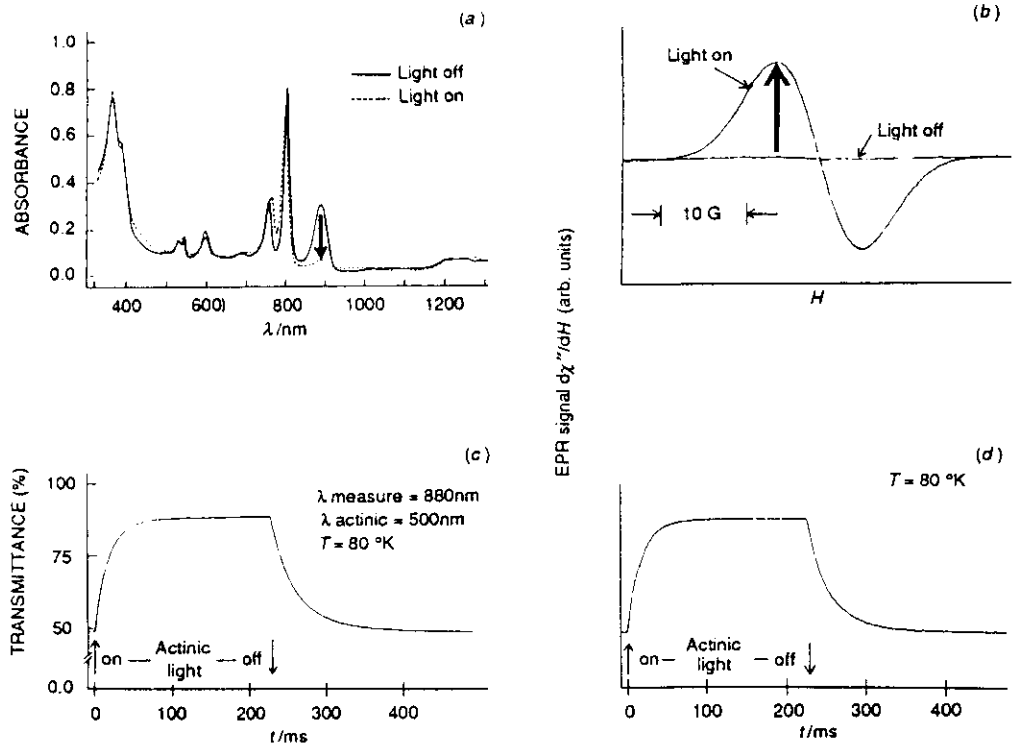

Fig. 6 Comparison of kinetics of the light-induced bleaching of the 865 nm peak (*a,c*) and the EPR signal (*b,d*) in RCs from *Rb. sphaeroides*. Top traces (*a, b*) show the steady-state spectra in the absence and presence of strong (actinic) illumination. Bottom traces (*c, d*) show the kinetics of charge separation and recombination. (*a*) T = 80 K; (*b*) T = 80 K, ν = 9 GHz; (*c*) T = 80 K, λ_{meas} = 880 nm, λ_{act} = 500 nm; (*d*) T = 80 K. Modified from McElroy *et al.*[10,11]

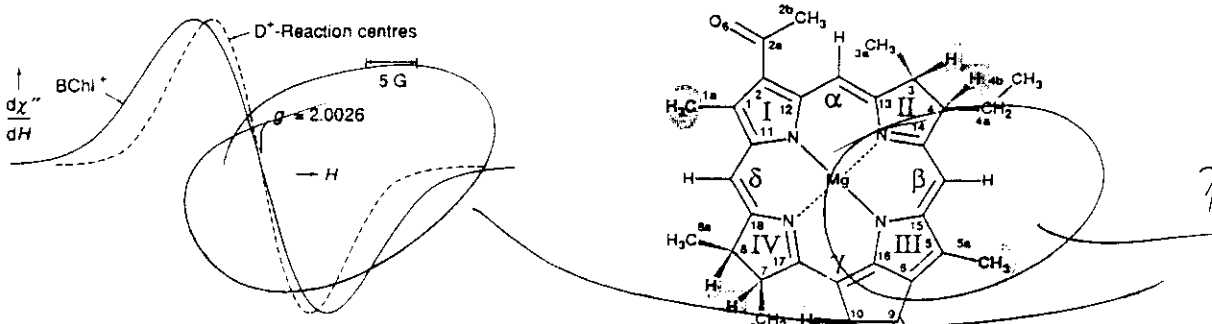

Fig. 7 Comparison of EPR lines from oxidized ($BChl^+$) *in vitro* and from illuminated RCs of *Rhodopseudomonas sphaeroides* R-26 (D^+) (T = 77 K ν_e = 9 GHz). From Feher *et al.*[13]

Fig. 8 Molecular structure and numbering scheme of BChl a. Protons removed by one C-bond from the conjugation (β-protons) are shown shaded. The side chain R is phytyl ($-C_{20}H_{39}$).

observed by Duysens long before RCs were purified.[7] When one switches from high to low light intensity the 865 peak recovers with a rate k_{AD} that is characteristic of the charge recombination.

$$D^+A^- \underset{k_{AD}}{\overset{k_{AD}}{\rightleftharpoons}} DA \qquad (2)$$

It is noteworthy that the charge separation and recombination occurs at cryogenic temperatures showing that we are dealing with a primary process. If one chemically oxidizes the RC the spectrum looks like that observed at high light intensity. We can ascribe, therefore, the bleaching of the 865 peak to the *oxidation* of D. The species most likely to absorb at 865 nm was believed to be some form of bacteriochlorophyll.

We now finally turn to EPR. The first photo-induced free radicals from green plants were observed by Commoner *et al.*[8] and from bacteria by Sogo *et al.*[9] These authors, however, did not identify the chemical origin of the signals. The EPR signal from RCs is shown in Fig. 5. This signal can be reversibly photo-induced at cryogenic temperatures. The same EPR signal is also observed when RCs are chemically oxidized. This suggests that the bleaching of the peak at 865 nm and the appearance of the

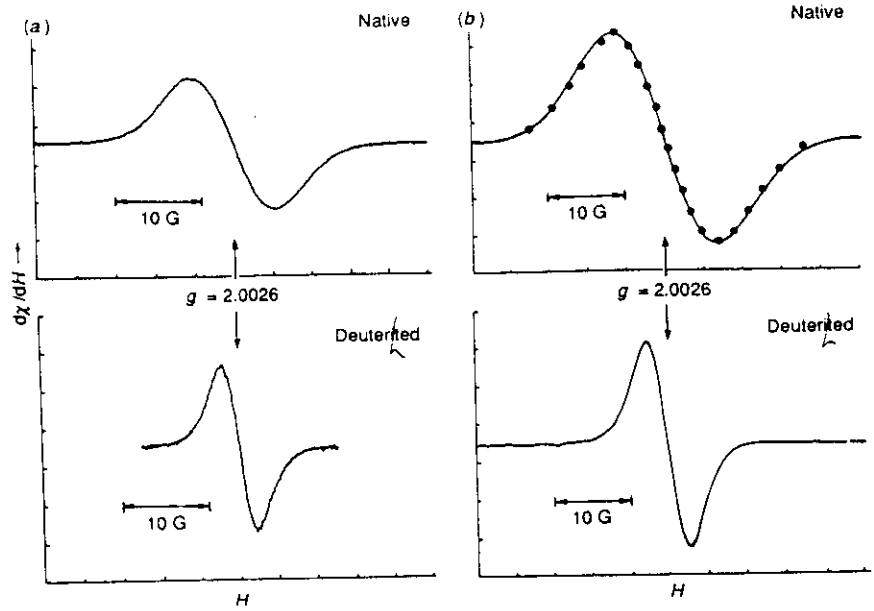

Fig. 9 EPR lines of the light-induced free radical in D^+ in reaction centres and the oxidized bacteriochlorophyll radical BChl at 9 GHz. The units of $d\chi''/dH$ are arbitrary. The points on the lines of the native radicals represent a Gaussian fit. From McElroy *et al.*[13] (*a*) *R. rubrum*; (*b*) oxidized BChl.

EPR signal are associated with the same process. To prove this identity, McElroy *et al.*[10,11] measured the kinetics of charge recombination by optical and EPR spectroscopy. Their results, presented in Fig. 6 show identical kinetics. Thus, the light-induced EPR signal and the optical bleaching of the 865 nm peak are associated with some (the same) form of oxidized bacteriochlorophyll.

The Model Compound Approach/ the Linewidth Puzzle.—Unfortunately EPR has not reached the stage where by inspection of a signal one can predict the chemical identity of the free radical. One resorts, therefore, to the model compound approach, *i.e.*, one prepares different radicals and compares their spectra with the unknown species. For a simple, structureless line like the one shown in Fig. 5 the two important parameters to be compared are the *g*-value and the linewidth.

From the results discussed in the previous section, the logical model compound to use for identifying D^+ was the cation of BChl. In other words, is eqn. (3) valid? Dave Mauzerall from the

$$D^+ \overset{(?)}{=} BChl^+ \qquad (3)$$

Rockerfeller University, who visited our lab in the late sixties prepared $BChl^+$ whose spectra we compared with D^+ in RCs.[10,12] The results are shown in Fig. 7. The g-values of the two lines are identical, suggesting that we were on the right track, *i.e.*, D^+ had something to do with $BChl^+$. Let me, therefore, remove one of the question marks in eqn. (3).

$$D^+ \overset{?}{=} BChl^+ \qquad (4)$$

However, the linewidth of the two radicals differ, their ratio being that shown in eqn. (5). Let us take a closer look at the

$$\frac{\Delta H(BChl^+)}{\Delta H(D^+)} = 1.4 \qquad (5)$$

problem of the linewidth. The width is due to the hyperfine (hf) interactions of the unpaired electron with the nuclei, *i.e.*, we are dealing with an inhomogeneously broadened line. The electron is delocalized over the π-system of the bacteriochlorophyll ring (Fig. 8) interacting with the H^1 and N^{14} nuclei. By growing the bacteria in D_2O and extracting the BChl from them, one observes a narrowing of the spectra of both D^+ and $BChl^+$ by a factor[12] of 2.5 ± 0.1 (Fig. 9). If the broadening were due only to protons one would expect a narrowing of a factor of 4.0. The smaller observed narrowing must, therefore, be attributed to interactions with other nuclei, most likely ^{14}N. The fact that the observed narrowing is the same in D^+ and $BChl^+$ further strengthens our belief that we are dealing with some form of BChl. We, therefore remove another question mark

$$D^+ \overset{?}{=} BChl^+ \qquad (6)$$

The remaining problem is the difference in linewidths.

Resolution of the Puzzle—the Bacteriochlorophyll Dimer.—So how do we account for the different linewidths? A number of ideas were put forward about different local environments, but the real answer was provided by Norris, Katz and coworkers[14] who postulated that the electron (hole) on D^+ is shared between two bacteriochlorophylls, *i.e.*, one deals with a bacteriochlorophyll dimer, the so called 'special pair.' Let us see in a simple way what the predicted narrowing in the dimer should be (for a more detailed treatment see ref. 14). The linewidth depends on the number of interacting nuclei, N, and the strength of their interaction A. For equivalent nuclei the width will be proportional to $A\sqrt{N}$; the square root arises from the random distribution of the orientation of the nuclei. If the electron is shared equally between the two halves of the dimer, it interacts with twice the number of nuclei, *i.e.*, N is doubled. However, the interaction A of the electron with each nucleus is halved since on the average the electron spends only half the time on each molecule. We can therefore write for the ratio of the linewidth of the monomer ΔH_m to that of the dimer ΔH_d, eqn. (7).

$$\frac{\Delta H_m}{\Delta H_d} = \frac{A_m\sqrt{N_m}}{A_d\sqrt{N_d}} = \frac{A_m\sqrt{N_m}}{\frac{1}{2}A_m\sqrt{2N_m}} = \sqrt{2} = 1.4 \qquad (7)$$

Data International Limited
Tue Sep 15 07 32 39 1992 perktwo p2r12424 5
123322 ch4036 total21081 wnvatt jn906786 PERK II Z/02500K 2/7

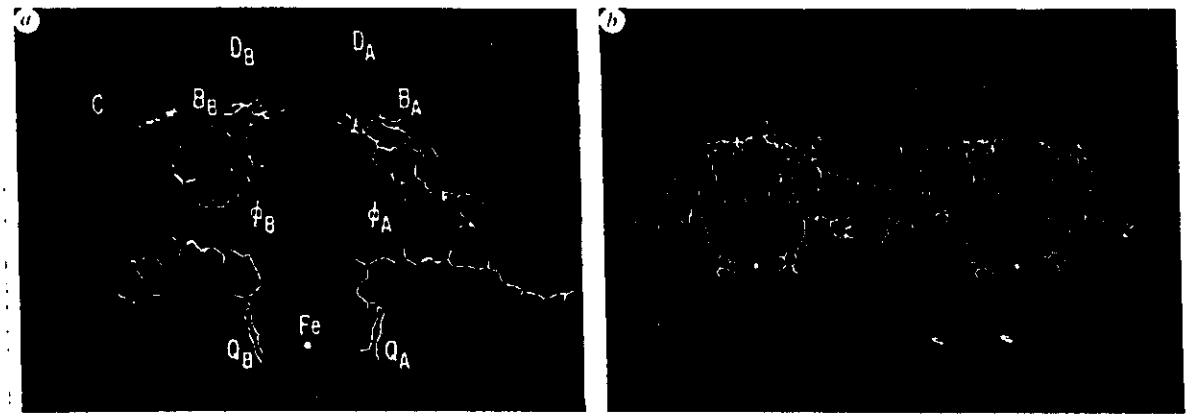

Fig. 11 Cofactor structure of the reaction centre from *Rb. sphaeroides*. (*a*) The symmetry axis is aligned vertically in the plane of the paper. (*b*) A stereo reconstruction rotated from the view in *a* by 90° clockwise around the twofold symmetry axis. The dimer structure of D is clearly seen in this view. Subscripts refer to the two branches A and B, sometimes also called L and M. Electron transfer proceeds preferentially along the A branch, except in the case of the dimer the electron can originate from either the A or B half of the dimer. The A-half of the dimer is defined as being closer to the L-subunit and the B-half closer to the M-subunit. [D_AD_B = $(BChl)_2$, B = BChl; ϕ = Bph, C = carotenoid]. From ~~Ivers~~ Feher *et. al.*[27]

(Facing p. 6)

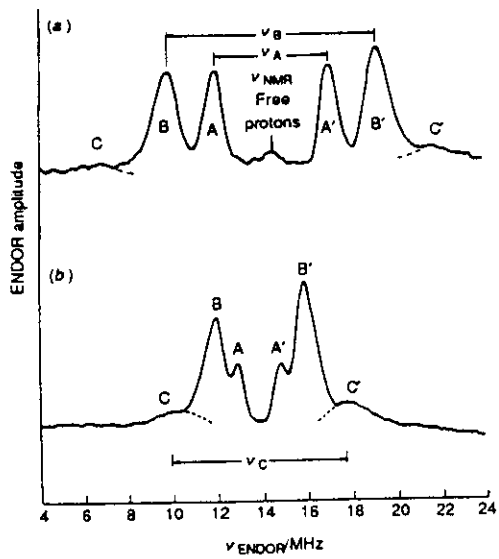

Fig. 10 Comparison of ENDOR spectra from $BChl^+$ *in vitro* (*a*) and chromatophores of *R. sphaeroides* R-26 (*b*). The hfs in chromatophores are reduced by a factor of *ca.* 2 as expected from the dimer model. From Feher *et al.*[13]

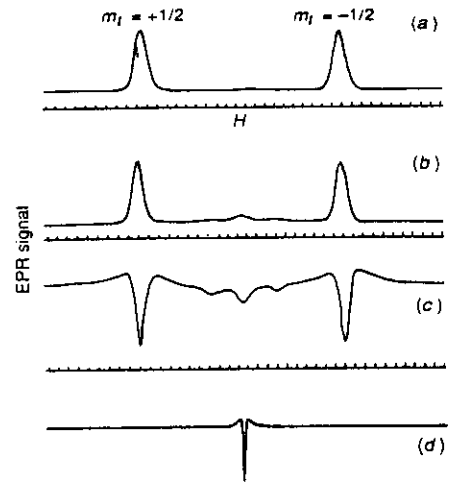

Fig. 12 EPR signal from silicon doped with varying concentrations of phosphorus donors. The range covers the transition from localized centres (*a*) to free carriers (*d*). For concentrations between these two extrema the observed resonance signal is due to clusters of donors (*b,c*) having their hf splittings reduced by $\frac{1}{2}$, $\frac{1}{3}$, *etc.* From Feher.[28] (*a*) 7×10^{15} P per cm^3; (*b*) 7×10^{16} P per cm^3; (*c*) 4×10^{17} P per cm^3; (*d*) 3×10^{18} P per cm^3

This is precisely the observed ratio [see eqn. (5)]. Is this numerology or is the dimer a reality? The question could be answered convincingly by showing that individual hyperline coupling constants A_i are halved in the dimer. This would eliminate the reliance on a single number. ENDOR provides the technique to measure the hfs A_i, and was applied to this problem.[13,15-17] Fig. 10 shows the comparison of ENDOR spectra from $BChl^+$ (*a*) and D^+ in chromatophores* (*b*) at 80 K. The general shapes of the spectra are similar except that the value of the hf splittings A, B and C in D^+ are approximately one half of those observed in $BChl^+$. Similar results were obtained by Norris *et al.*[16,17] This, then, validates the dimer model, eqn. (8).

$$D^+ = (BChl)_2^+ \qquad (8)$$

Note that the dimer is not covalently bound and when extracted with organic solvents falls apart and is indistinguishable from the other bacteriochlorophyll monomers in the RC. Biochemical techniques would therefore not have been useful to prove the identity of D. There is, however, an even more powerful technique than EPR, by which structures can be determined and that is X-ray diffraction. Unfortunately, there are some hurdles to be overcome before this technique can be applied.

Confirmation of the Dimer Structure by X-Ray Diffraction.—A requirement for the determination of the three-dimensional structure of macromolecules is the availability of relatively large, well-ordered single crystals. Michel was the first to succeed in crystallizing RCs from the bacterial species *Rps. viridis*.[18] Soon thereafter RCs from *Rh. sphaeroides* were crystallized[19,20] and the three-dimensional structure of both RCs were determined.[21-26] The structure of the cofactors is shown in Fig. 11.[27] The dimeric nature of D is clearly discernible; the two halves D_A and D_B overlap at ring I (see Fig. 8). It is gratifying to see the structure deduced from EPR and ENDOR experiments to be conclusively confirmed a decade later.

Having identified D^+ as a BChl dimer, the next goal was to investigate its electronic structure. To this end we needed to assign the ENDOR lines to specific protons and to compare the hfs to theoretically calculated spin densities.

Before discussing these points I would like to make a retrospective (introspective) remark concerning the narrowing of interacting molecules. In one of my previous lives many years ago I investigated EPR spectra of donors in silicon.[28] When the concentration of the donors was increased, they interacted with each other and hfc splittings whose values were $\frac{1}{2}$, $\frac{1}{3}$, *etc.* were observed (Fig. 12). At very high concentrations the electron was completely delocalized giving rise to a narrow EPR line. Although this situation is not exactly analogous to the bacteriochlorophyll case,† it should have rung a bell when a decade later we saw the narrowed line. That it did not, shows the sad limitation and compartmentalization of one's (my!) brain.

The Electronic Structure of the Primary Donor

ENDOR/TRIPLE of $BChl^+$ and RCs in Solution.—Having identified the primary donor as a BChl dimer, the next task was to investigate its detailed electronic structure. To accomplish this it was necessary to assign the observed ENDOR lines to specific protons. Let us start with the three sets of lines observed in frozen solutions (Fig. 10). The first question to be answered is why we see only three sets of lines, *i.e.*, where are the ENDOR lines due to the rest of the dozen or so protons that presumably interact with the unpaired electron. The answer lies in the anisotropic (dipolar) part of the hf interaction which in frozen solution causes an excessive broadening. Protons that are removed by one carbon bond from the conjugated ring (β-protons) are expected to have smaller anisotropic hfs than protons adjacent to the ring (α-protons).[30] There are seven

* Chromatophores are closed plasma membrane vesicles that form when the bacterium is broken up. Purified RCs from *Rh. sphaeroides* gave spectra that were similar to those observed from chromatophores.

† In the $(BChl)_2$ case the electron is shared between the two molecules. In the donor case there are two (or more) electrons that interact with each other.[29]

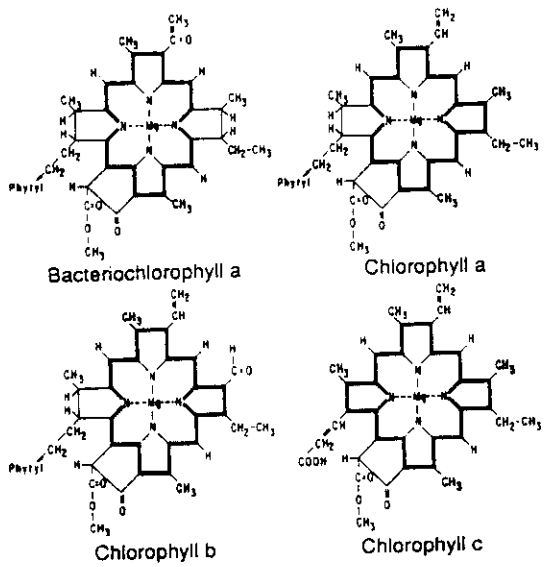

Fig. 13 The structure of bacteriochlorophyll a, chlorophyll a, b, and c. Heavy lines indicate the conjugation paths; shaded circles emphasize the methyl group that play a special role in the ENDOR experiments. From Feher *et al.*[13]

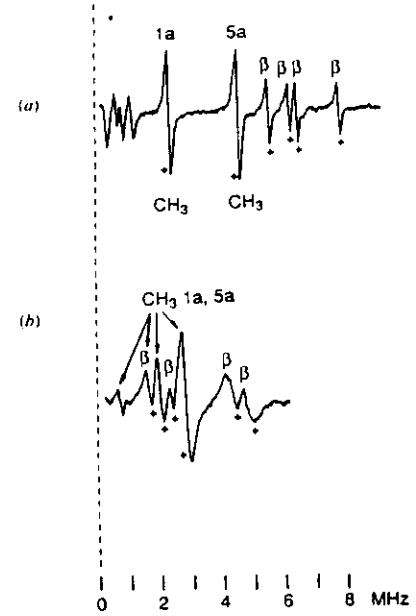

Fig. 14 ENDOR/TRIPLE spectra of $BChl^+$ in CH_2Cl_2 CH_3OH, 255 K (*a*) and D^+ (alternative nomenclature P^+_{865}) in RCs from *Rb. sphaeroides* in H_2O, 293 K (*b*). Modified from Plato *et al.*[35]

groups of β-protons in $BChl^+$ shown shaded in Fig. 8. The $-CH_3$ protons are expected to give the largest ENDOR signal since the three protons are still rotating in frozen solutions making them magnetically equivalent. Furthermore their anisotropies are expected to be smaller than those of the β-protons on rings II and IV. Consequently, we assign lines A and B in Fig. 10 to the $-CH_3$ groups on rings I and III and line C to β-protons on rings II and IV. This assignment was confirmed by selective deuteriation of the β-protons on rings II and IV.[31] The ENDOR spectrum in these deuteriated samples lacked line C.[13] The hfs of the β-proton at position 10 (Fig. 8) is expected to be small and not to contribute to the ENDOR spectrum.[17,32]

The question that remained to be answered is which of the ENDOR lines (A, B in Fig. 10) belong to which $-CH_3$ groups. This was accomplished by obtaining the ENDOR spectrum from cation radicals of chlorophylls having different numbers of methyl groups (Fig. 13). All of them show two sets of sharp lines analogous to A and B in Fig. 10. The ratio of amplitudes of the A set to the B set of lines increased monotonically on going from chlorophyll b to chlorophyll a to chlorophyll c. Assuming that the methyl group on ring III, adjoining the symmetry-breaking ring V, exhibits a different hf interaction from the other, quasi-equivalent CH_3 groups, the observed amplitude ratios indicate that the larger (B) splitting is due to the $-CH_3$ group on ring III.[13] Norris *et al.* using a different method arrived at the same conclusion.[17]

From the above discussion it is clear that if we wish to obtain the hfs of the other protons, we need to eliminate the broadening of the ENDOR lines due to the anisotropic part of the hf interactions. This is attained by performing the experiments in liquid solutions, in which the molecules (proteins) tumble faster (*i.e.* have a shorter correlation time) than the inverse hf interaction frequency. Consequently, the anisotropic, dipolar interactions average to zero and narrow lines are obtained. Experiments of this nature were first performed on $BChl^+$ by Borg *et al.*[33] and on D^+ by Lendzian *et al.*[34] Fig. 14(*a*) shows the results for BChl *a*$^+$. The four β-protons on rings II and IV, as well as the two assignment was again based on isotopic substitution experiments as well as on theoretical MO calculations.[32] Note that the results shown in Fig. 14[35] were obtained with a technique that is a modification of the standard ENDOR method, the so-called special TRIPLE in which two NMR frequencies corresponding to the low and high frequency ENDOR transitions are applied simultaneously.[36,37] In this technique the observed transitions occur at one half the hf. The advantage of this technique has been discussed elsewhere.[38] The sign of the isotropic hf coupling has been obtained by saturating (pumping) specific ENDOR transitions and observing the effect on the amplitude of other ENDOR transitions.[38,39] This technique is called general TRIPLE.[37] Often the sign can be obtained simply from the ratio of amplitudes of the high-frequency ENDOR lines.[40]

The ENDOR/TRIPLE spectrum of D^+ (also called P^+_{865}) together with some tentative assignments is shown in Fig. 14(*b*). Since the hf are reduced on the average by a factor of *ca.* 2, the spectrum is more crowded and the assignment becomes more difficult. The difficulty is further compounded by the fact (to be discussed in more detail later) that the spin densities are not distributed symmetrically over the two halves of the dimer. Consequently, the number of ENDOR lines is doubled. This poses the additional problem of knowing which lines belong to which half of the dimer. In the past this problem has been tackled, with partial success, by theoretical calculation.[35] The experimental approach to the solution of this problem is to work on single crystals of RCs.

ENDOR/TRIPLE on Single Crystals of Native RCs.—In frozen solutions the random orientation of the molecules (each with a different hfc) causes a broadening of the ENDOR lines. In contrast with frozen solution, the ENDOR lines in liquid solutions are narrow and hence better resolved. However, one

Strictly speaking, most of the work has been performed on a carotenoidless mutant R-26. However, its main structure is, within the resolution of the X-ray diffraction, indistinguishable from the native 2.4.1

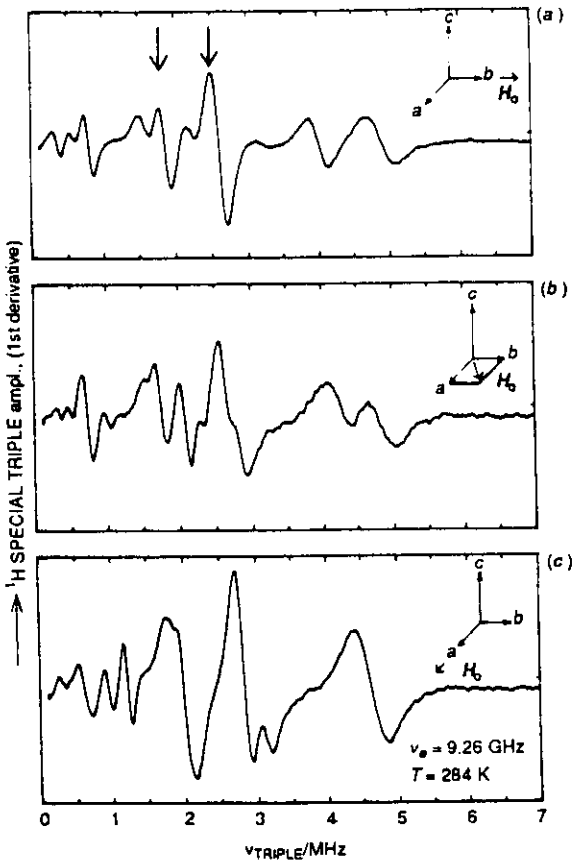

Fig. 15 ENDOR/TRIPLE spectra of D^+ in single crystals of *Rb. sphaeroides* RCs with $H_0 \| b$ axis. (a), $H_0 \| a$ axis (c) and with H_0 45° from both axes (b). From Lous *et al.*[42]

pays a price for the higher resolution: information concerning the magnitude of the anisotropic part of the hfs is lost. This information can be retrieved by working with single crystals, where the molecules are ordered and the broadening due to anisotropies does not occur. An additional important advantage of single crystals is that the observed anisotropies can help in the assignment of the ENDOR lines to specific nuclei. This comes about in the following way: Experimentally we can determine the directions of the principal axes of the hfs tensor. The direction of the largest hfs is expected to lie close to the C–H bond direction. From the known structure we can calculate the directions of the components of the hfs tensor and compare them with the observed values.

ENDOR/TRIPLE spectra of D^+ on single crystals of RCs from *Rb. sphaeroides* R-26 at 284 K were obtained independently by the San Diego[42] and Berlin[43] groups. The results are shown in Fig. 15 for three directions of H_0 in the *ab*-plane of the crystals. A complication encountered in the single crystal work is that there are four RCs per unit cell (space group $P2_12_12_1$). Thus, in an arbitrary direction of the magnetic field, H_0, with respect to the crystal axis, the number of ENDOR lines should be four times larger than observed in a single dimer. Fortunately when H_0 lies in one of the principal planes, the RCs are pairwise magnetically equivalent and one expects only two sets of ENDOR/TRIPLE lines for each group of protons. When H_0 points along a principal axis, all four RCs are magnetically equivalent and one obtains a single ENDOR/TRIPLE line for each proton. This situation is illustrated in Fig. 16. The top shows a stereoview of the unit cell with its four bacteriochlorophyll dimers. The bottom is a projection on the *ab* plane showing the pairwise equivalence of the dimers. The angle between the C–CH_3 bonds of the magnetically inequivalent sites are shown for the methyl $5a_A(\Delta\Psi_A)$ and $5a_B(\Delta\Psi_B)$.

The detailed angular dependence of the hf splittings, with H_0 rotated in the three principal crystallographic planes *ab*, *ac*, and *bc*, is shown in Fig. 17.[44] For most ENDOR transitions two sets of lines corresponding to the two inequivalent sites are clearly discernible. When the splittings between the two sites are smaller than their linewidths only one broadened line is observed (*e.g.* line 3_A in the *ab* plane). The solid lines in Fig. 17 are theoretical fits to eqn. (9)[44] where A_{ii} and A_{jj} are the

$$\nu_{TRIPLE} = \tfrac{1}{2}|A_{ii}\cos^2\varphi + A_{jj}\sin^2\varphi + 2A_{ij}\sin\varphi\cos\varphi| \quad (9)$$

diagonal and A_{ij} the off-diagonal elements of the hfs tensor in the coordinate system of the crystal axes, and φ is the angle of the magnetic field of H_0 with respect to the *i*-axis. Note that the diagonal elements are determined from the positions of the ENDOR/TRIPLE lines along the symmetry axes *a*, *b*, *c*.

Let us now briefly consider the assignments of the main ENDOR/TRIPLE lines (for a more detailed discussion see ref. 44). As mentioned earlier the narrowest and most intense lines are expected from the CH_3 groups 5a and 1a (Fig. 8). They are indicated by arrows in Fig. 15 and correspond to hfs of *ca.* 4 and *ca.* 5.5 MHz. The two sets of lines exhibit the *same* angular dependence (Fig. 17). Since the C–CH_3 bond directions of 5a and 1a in a bacteriochlorophyll monomer are approximately parallel, the two sets of lines must originate from the *same half* of the dimer. To determine to which half they belong, we compared the direction of the largest value of the diagonalized hf tensor with the directions of the C–CH_3 bonds on the A and B half of the dimer. The difference in directions was found to be much smaller for the A half of the dimer. Consequently, the lines are assigned to $5a_A$ and $1a_A$, the larger hfs being assigned to 5a as discussed earlier. The lines associated with the CH_3 groups on the B half of the dimer have been tentatively assigned as indicated in Fig. 17.[44]

The largest hfs are expected from the β protons on rings II and IV (Fig. 8). This conclusion follows from ENDOR work on monomeric $BChl^+$ *in vitro* (Fig. 14) and from theoretical calculations.[32,33,35] Following the procedure outlined in the previous paragraph, *i.e.*, comparing the directions of the experimental and calculated principal axes of the hfs tensor, the lines were assigned to protons 4_A and 3_A of ring II (although the assignment to 7_A and 8_A cannot be entirely excluded).

The splittings with the largest anisotropies are expected to arise from π-protons, *i.e.*, the methine protons α, β, δ (Fig. 8). Their assignment shown in Fig. 17 was obtained by procedures similar to those discussed above.[44]

ENDOR/TRIPLE on Single Crystals of Mutant (Heterodimer) RCs.—Mutations of amino acid residues in the vicinity of the primary donor, D, cause changes in the electronic structure with concomitant changes in function, *i.e.*, changes in electron transfer characteristics. Thus, site-directed mutagenesis provides a powerful tool for investigating the relationship between structure and function.

Two mutations seem particularly interesting with respect to the primary donor. They involve the two histidines whose nitrogens can form ligands to the central Mg atoms of the two halves of the bacteriochlorophyll dimer (Fig. 18).[45,46] In one mutant, HL (M202), the histidine at position M202 was replaced and in the other mutant, HL (L173), the histidine L173

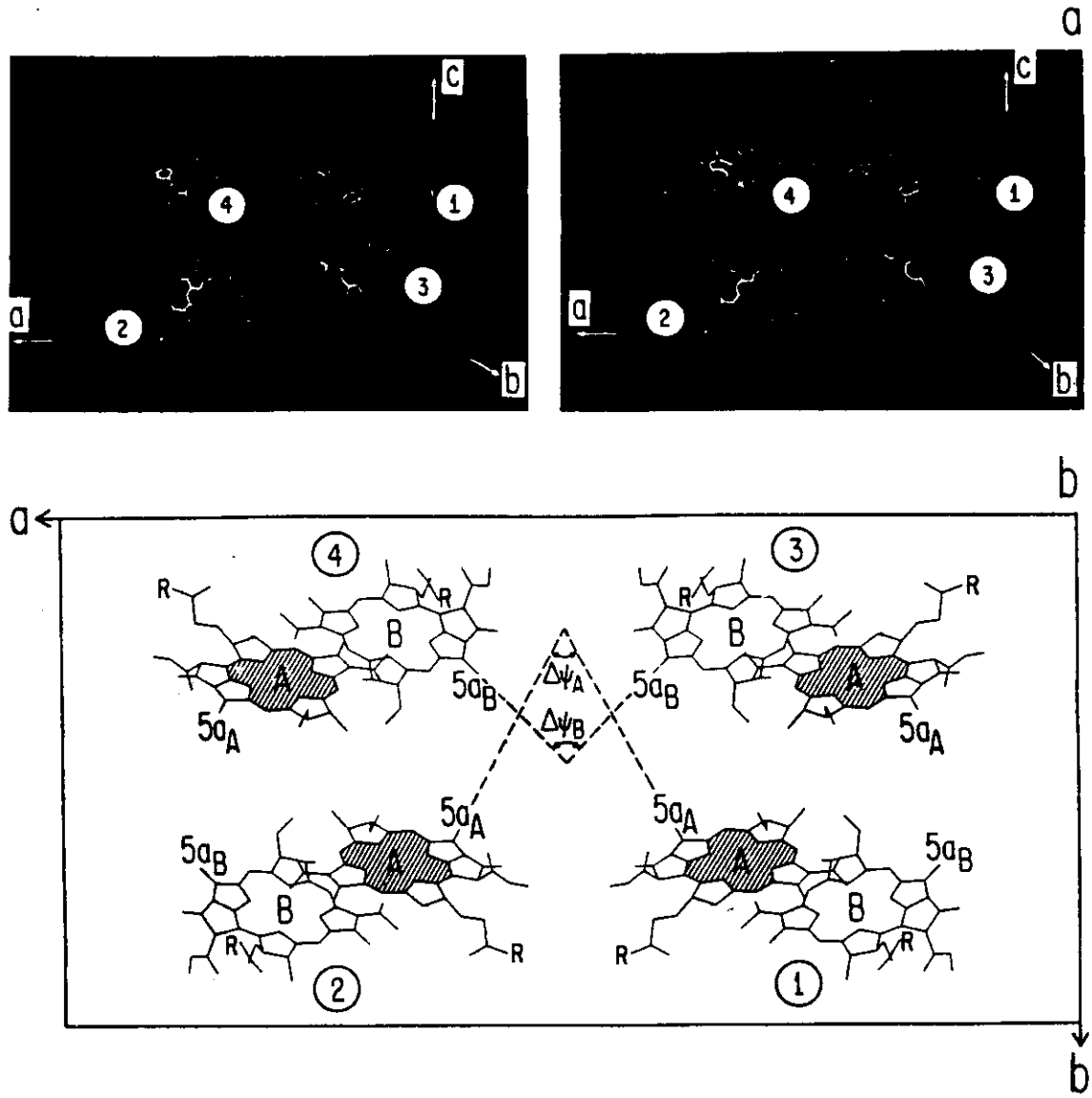

Fig. 16 (*a*) Stereoview of the bacteriochlorophyll dimers of the four symmetry-related RCs in the crystal with respect to the crystallographic axis system (sizes of molecules and distances between individual Ds are not drawn to scale). (*b*) Projections of Ds onto the *ab* plane. Note that dimers 1 and 3 (as well as 2 and 4) are related by a twofold symmetry axis and should, therefore, be magnetically equivalent. With $H_{rf} \| a$ or $H_{rf} \| b$ all four Ds are magnetically equivalent. The angle between the C–CH_3 bonds of the magnetically inequivalent sites are shown for the methyl group $5a_A$ ($\Delta\Psi_A$) and $5a_B$ ($\Delta\Psi_B$). For simplicity the phytyl chains were truncated and their positions denoted by R. From Lous *et al.*[41]

(Facing p. 8)

Data International Limited
Tue Sep 15 07 54 48 1992 perktwo pZr12424 -16
123322 ch744 total62111 whyatt jn906788 PERK II 2/02500K 2/7

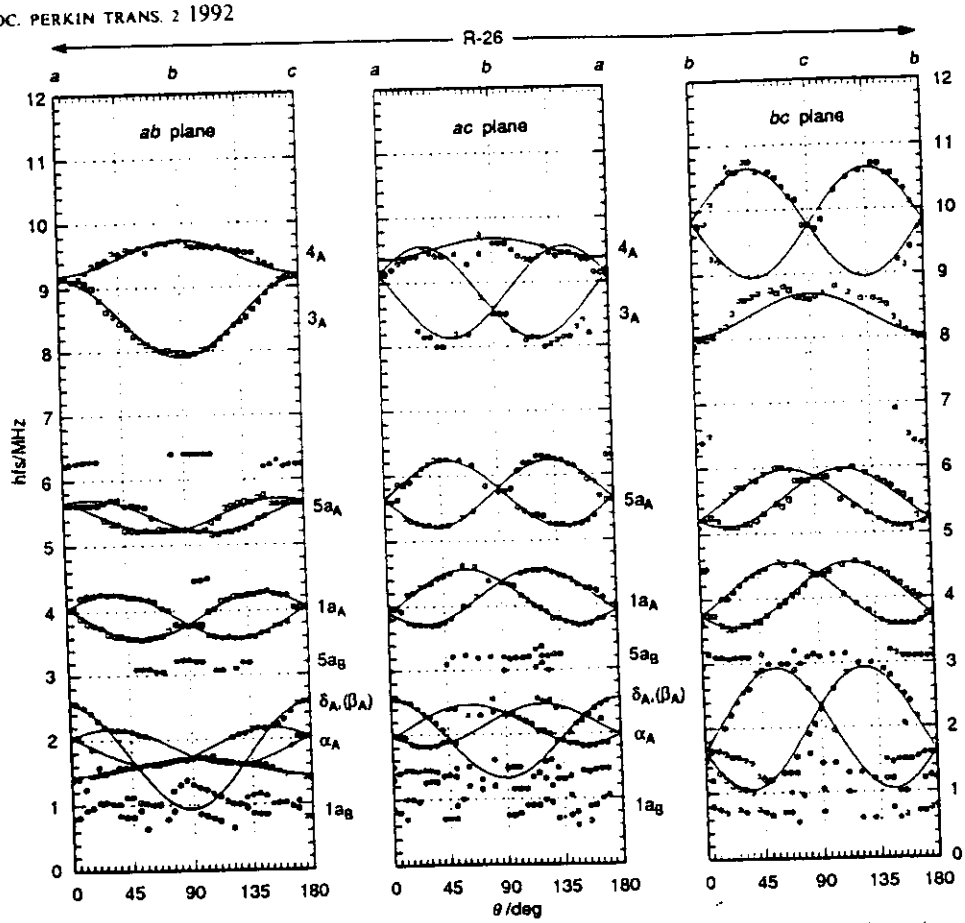

Fig. 17 ENDOR/TRIPLE spectra in single crystals of RCs from *Rb. sphaeroides* R-26 in the three principal symmetry planes *ab*, *ac* and *bc*. Circles are experimental points, solid lines represent fits to eqn. 9. Numbers at the side of the lines refer to assigned proton positions. Some of the assignments, in particular at the low frequencies, should be regarded as tentative. Modified from Lendzian *et al.*[44]

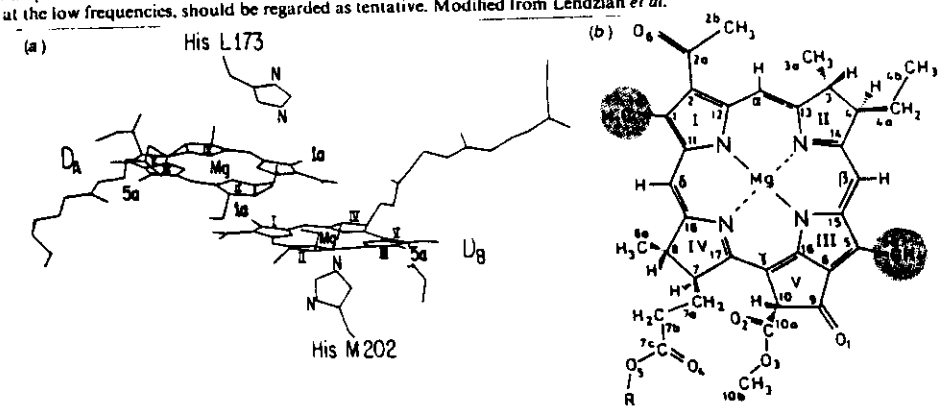

Fig. 18 (*a*) Structure of the primary donor D in RCs of *Rhodobacter sphaeroides* (coordinates from ref. 45). The phytyl side chain has been partially truncated. (*b*) Molecular structure of BChl a with numbering scheme. The methyl groups 1a and 5a, which were investigated in detail, are shaded. The side chain R is phytyl ($-C_{20}H_{39}$). From Huber *et al.*[46]

was replaced by leucine,[47] a residue that cannot act as a ligand to Mg.* Analogous mutants have been previously reported in *Rb. capsulatus*.[48] In these mutants the BChl close to the site of the mutation is replaced by bacteriopheophytin (BPhe).[47,48] Thus, in the HL (M202) mutant, D_A is a BChl and D_B a BPhe, whereas in the complementary mutant HL (L173) it is the other way around. The special pair in these mutants is, therefore, called a heterodimer. The photophysical changes observed in the heterodimers of *Rb. sphaeroides* have been discussed by

* In RCs from *Rb. sphaeroides* the distance of His L173 to Mg has been reported to be too large (4 Å) for histidine to be a ligand to Mg.[45] In the recently refined structure of the RC, this distance is 2.7 Å (4RCR structure, available from Brookhaven databank).

Datax International Limited
Wed Sep 16 09:38:25 1992 perktwo p2r12424 -9
123322 ch1576 total1576 jn

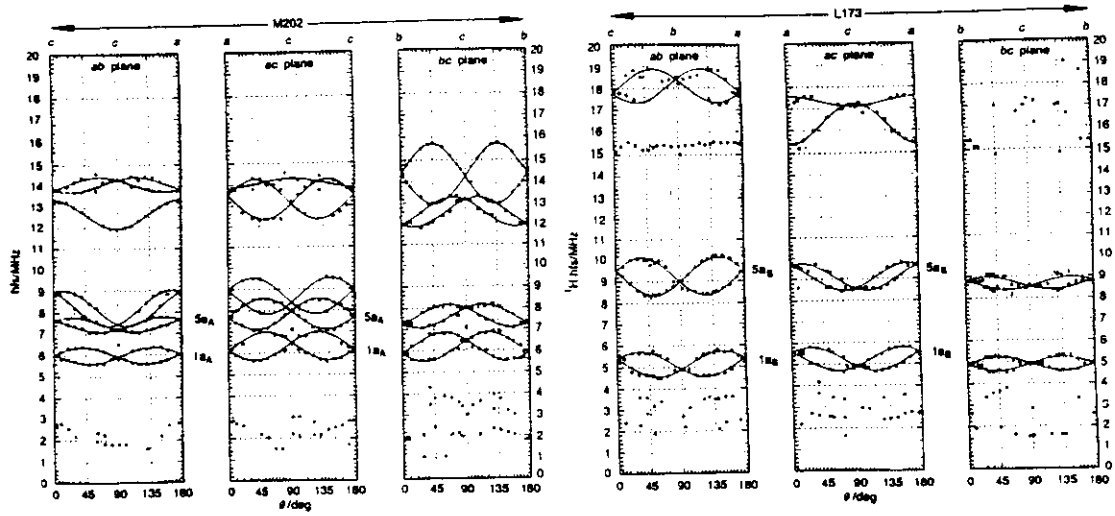

Fig. 19 Angular dependence of the hfs of D^+ in single crystals of the two heterodimer mutant RCs: HL (M202) and HL (173). Hfs are plotted *vs.* the angle between the externally applied magnetic field H_0 and the crystallographic axes in the *ab*, *ac* and *bc* planes. Circles are experimental points, solid lines are fits to eqn. (9). T = 284 K, $\nu_e \cong$ 9.6 GHz. From Huber *et al.*[51]

McDowell *et al.*[47] The most important finding is that the rate of the first (picosecond) electron transfer in the heterodimers is reduced by approximately one order of magnitude with a concomitant *ca.* 50% reduction in quantum yield. However, the unidirectionality of the electron path along the *A*-branch remained unaffected.

The EPR linewidth of D^+ in the heterodimer mutants is *ca.* 13 G (peak-to-peak derivative),[46,49] which is close to that of the $BChl^+$ monomer.[10,12] This indicates that, in contrast with wild-type RCs, the electron in the mutants is localized on one half of the dimer, making it effectively a monomer. This is not surprising in view of the difference in redox potentials between BChl and BPhe; BChl being easier oxidized than BPhe.[50] Thus, in the HL (M202) mutant the unpaired electron is localized on D_A, whereas in the HL (L173) it is localized on D_B.

The ENDOR/TRIPLE results on the heterodimer mutants are shown in Fig. 19.[51] Although the general pattern is similar to that obtained on R-26 (Fig. 17), the values of the hfs are considerably larger in the mutant, as would be expected from the localization of the electron.

To obtain a picture of the spin-density distribution in the bacteriochlorophyll macrocycles, let us focus on the hfs of CH_3 groups on rings I and III (positions 1a and 5a, respectively; Figs. 8 and 19). Fig. 20 summarizes the results obtained on the native homodimer, the two heterodimers and the $BChl^+$ monomer.

The following conclusions can be drawn. (*i*) The electron distribution in the homodimer structure of R-26 is asymmetric, favouring the A side by a ratio of *ca.* 2:1. (*ii*) The sum of the spin densities $\Sigma A_i(CH_3)$ is approximately constant for all the structures. (*iii*) There is a significant difference in the spin density distribution in the two heterodimers. (*iv*) The spin density distribution in the heterodimers [in particular HL (L173)] differs significantly from the distribution of the spin densities in the respective halves of the homodimer. (*v*) The spin density distribution in the HL (L173) mutant is closer to that of the $BChl^+$ monomer (in an organic solvent) than to the distribution in the HL (M202) mutant.

These conclusions point to the fact that the spin densities are significantly affected by the protein environment and by interactions between the two dimer halves. Consequently, it is more appropriate to view the dimer as a supermolecule rather than a system of two weakly interacting BChls.

A word needs to be said about the seeming inconsistency between the asymmetric spin density in the native dimer and the observed narrowing of the linewidth by $\sqrt{2}$. Eqn. (7), which predicts the $\sqrt{2}$, was derived under the assumption of a symmetric spin-density distribution. In the presence of an asymmetry, the narrowing factor is expected to be smaller than $\sqrt{2}$, in contrast with the observed value [eqn. (5)]. Apparently, in the case of *Rb. sphaeroides* there is a reduction in the hfs of the β-protons on ring II and IV that fortuitously restores the $\sqrt{2}$.[44] In another bacterial species, *Rps. viridis*, the observed reduction factor in linewidth is only 1.17.[52] In that species the fortuitous cancellation does not occur. It is fortunate that *Rb. sphaeroides* was the first species to be investigated in detail. Had it been *Rps. viridis*, it is doubtful whether the dimer hypothesis would have been advanced at that stage.

^{14}N, ^{15}N and ^{25}Mg ENDOR.—The spin of the unpaired electron in $BChl^+$ and D^+ interacts not only with protons but also with the four nitrogen nuclei and the central magnesium atom. The small size of the magnetic moment of the naturally occurring (99.6%) ^{14}N as well as its quadrupole moment makes the observation of ^{14}N ENDOR difficult. Consequently, ^{14}N was replaced by the more favourable nucleus ^{15}N ($I = \frac{1}{2}$) by growing *Rb. sphaeroides* in an ^{15}N-enriched medium.[53]

Our main motivation of the ^{15}N ENDOR work came from a theoretical suggestion by O'Malley and Babcock,[54] who claimed to explain the EPR and ENDOR data with a monomer model. The essence of their model was a mixing by the RC protein of the ground state with the first excited doublet state of D^+ leading to a hybrid orbital in the monomeric $BChl^+$ in which the unpaired electron is delocalized. The model predicts the sign of the ^{15}N hfs to be the opposite of that predicted by the dimer model. Thus, doubt was cast on the dimer model just prior to the X-ray determination of the structure.[21,22]

In liquid solutions four ^{15}N ENDOR lines were observed in both the $BChl^+$ and D^+, with an average reduction factor of the hfs in D^+ by *ca.* 2. The sign of the hfs in D^+ was determined by the general TRIPLE method to be in agreement with the dimer

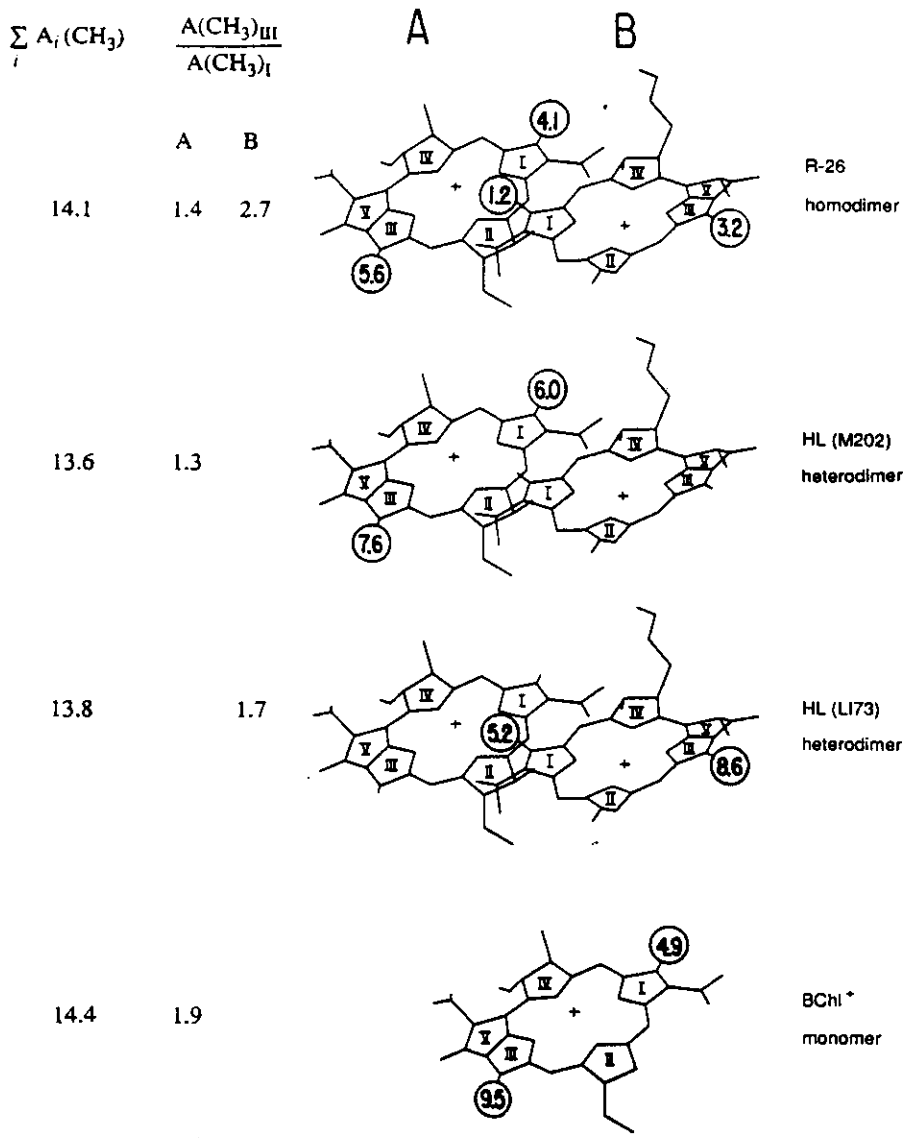

Fig. 20 Comparison of the isotropic hfs (in MHz) of the CH_3s on rings I and III in the native homodimer (top), mutant heterodimers HL (M202), HL (L173) and monomer $(BChl)^+$

model.[53] Similar results were later obtained from electron spin echo modulation experiments by De Groot *et al.*[55]

In frozen solution an attempt was made to determine the anisotropic part of the hfs. However, some broad lines were missed, as pointed out by Lin and Norris[56] in a subsequent electron spin echo modulation investigation.

In these early experiments [53,55,56] a symmetric dimer was assumed, which we now know to be incorrect. Recent experiments by Lubitz, Lendzian *et al.* on D^+ in single crystals of ^{15}N-enriched RCs provide an estimate of all eight ^{15}N hfs tensors.[57] Their results point again to an asymmetric spin density distribution, favouring the A-side by a factor of *ca.* 2:1.

ENDOR experiments on ^{25}Mg ($I = 5/2$) are even more difficult than on ^{15}N. In addition to the quadrupole moment of ^{25}Mg and its small magnetic moment, the spin density at the centre of the ring is expected to be small. Nevertheless, ENDOR spectra were obtained on the $BChl^+$ monomer.[58] The hfs was determined to be −0.3 MHz. So far no ENDOR results have been reported on D^+.

Comparison of the Observed Hyperfine Couplings with Theoretical Calculations.—To relate the observed hfs to structural properties in a quantitative way, molecular orbital (MO) methods were used to calculate spin densities on $BChl^+$ and the oxidized bacteriochlorophyll dimer D^+ (reviewed in ref. 59). The latest results obtained by Plato[44,60] for the spin density using a semiempirical all-valence-electron MO method RHF-INDO/SP (Restricted Hartree–Fock Intermediate Neglect of Differential Overlap/Spin Polarization) in conjunction with the X-ray structure analysis[45] is shown in Fig. 21. The agreement of theory with experiment is quite good, including the observed asymmetry in the spin densities on the two halves of the dimer. The calculations show that there is a strong π–π interaction between the halves resulting in 'super'

Data International Limited
Tue Sep 15 07:50:11 1992 perktwo p2r12424 11
122322 ch2087 total:44942 whv:11 in:906786 PERK II 2 02500K 2 7

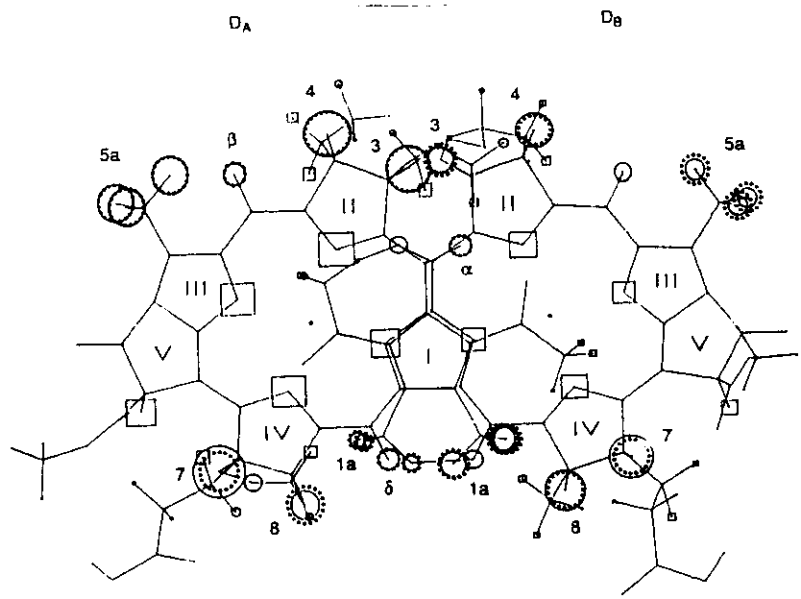

Fig. 21 Comparison of experimental (····) and calculated ⊗ spin densities (——) of D^+ in *Rb. sphaeroides* R-26. ⊗ Spin densities are proportional to the areas of the squares ($\rho < 0$) and circles ($\rho > 0$). Geometry from X-ray structure analyses.[43] From Lendzian *et al.*[44]

MOs that extend over the entire dimer. In such a supermolecule the contribution of the monomers to the total wavefunction depends sensitively on the details of the structure. Relatively small distortions brought about by the protein environment can lead to large changes in spin densities. For instance, the main contribution to the asymmetry can be traced back to the different orientations of the acetyl groups (see Fig. 8, ring I) on D_A and D_B. It also points to the importance of trying to decrease the errors in the coordinates obtained from the X-ray diffraction analysis. It is this sensitivity to structural detail that may be responsible, to a large extent, for the different predictions of spin densities in the past.[39] For instance, there is a significant discrepancy between the spin densities shown here in Fig. 21 and in Fig. 10 of ref. 59. One should, therefore, be prepared for further modifications in the calculated ⊗ spin densities as the structure analyses and computations improve. The directions of the principal axes of the hfs tensors were obtained from the p_z-spin densities (not shown).[44] These directions are less sensitive to structural details than the ⊗ spin densities.

Summary and Discussion

We have shown how EPR and ENDOR have been used to establish that the identity of the primary donor in bacterial photosynthesis is a BChl dimer. The same tools were then applied to the elucidation of the electronic structure of the dimer. ENDOR provided the means of mapping the spin density distribution of D^+ and of assessing the effect of the protein environment on the electronic structure. Experiments on single crystals of native and site-directed mutant reaction centres (heterodimers) helped to identify individual ENDOR lines with particular protons. The results showed that the spin density is asymmetrically distributed in the native dimer, favouring the A-half by *ca.* 2:1.

The experimentally determined spin densities and derived wavefunctions are important in understanding the mechanisms and kinetics of electron transfers which constitute the basic primary processes of photosynthesis. In addition, they serve to test the reliability of modern molecular orbital calculations, which can be used to predict other properties (*e.g.*, optical spectra) of the reaction centre.

Before concluding, may I indulge in a bit of speculation. The question that I would like to address is: why did nature pick a dimer for the primary donor?

There does not seem to be a simple, clear, answer to this question, indeed several possible explanations exist. The simplest one involves the shift of the singlet optical absorption of the dimer to a lower energy (red shift).* This provides a natural trap for funnelling the light energy from the light harvesting bacteriochlorophylls to the reaction centre. However, this does not seem to be an absolute requirement for the organism to survive. There are species (*e.g. Rps. viridis*) in which the light-harvesting BChl absorbs at a longer wavelength than the RC. But in this species the efficiency of energy transfer from the light-harvesting BChl to the RC is significantly reduced.[61]

Another point deals with the utilization of the incoming photons. If the primary donor were a monomer it would be indistinguishable from the monomer B_A (see Fig. 11). Consequently, a photon could be absorbed with equal probability by either the donor or B_A. But a photon absorbed by B_A would produce an inefficient charge separation and would, therefore, be essentially wasted.

The other explanations deal with the optimization of electron transfer. We require a fast forward and slow back reaction (Fig. 2). The forward reaction is optimized if the reorganization energy, λ, equals the energy difference, ΔG, between the reactant and product states (for a review see ref. 62). We do not want ΔG to be large since this would represent a loss in energy; consequently we want also a small reorganization energy. A large structure, like the dimer with its delocalized charge distribution, will have a lower reorganization energy than a monomer, and

* Two interacting molecules will, in general, have their energies split; one energy level will be lowered, the other raised. The bleachable 865 nm band in RCs (see Fig. 4) is due to the lower energy transition; the higher energy transition presumably hides underneath the 800 nm band.

Dalrx International Limited
Tue Sep 15 07 50:13 1992 perktwo p2r12424 -12
123322 ch4615 total49557 whvatt jn906788 PERK II 2/02500K 2/7

will therefore more easily satisfy the matching condition discussed above.

An important factor in the energetics of electron transfer is the difference in redox potentials between a bacteriochlorophyll dimer and a monomer; the dimer is oxidized more easily than the monomer by *ca.* 0.2 eV.[50] This probably accounts for the major part of the reduced primary electron-transfer rate and concomitant reduced quantum yield in the heterodimer, which behaves essentially like a monomer.[47]

In addition to the energetics discussed in the previous paragraph, dynamics play an important role in electron transfer. The dimer is a floppy structure that has many low frequency modes. These modes will broaden the energy levels of the reactant and product states, facilitating an overlap between them that is necessary for efficient electron transfer.

To speculate one step further, let us ask whether there might be an additional advantage to having an *asymmetric* dimer. Consider the following situation. Light excites an electron into the lowest unoccupied orbital (LUMO) leaving an unpaired electron (actually a hole) in the highest occupied orbital (HOMO). Suppose that in an asymmetric dimer the hole resides preferentially on the half of the dimer that is unfavourably situated with respect to charge recombination (back reaction), whereas the electron in the LUMO is localized preferentially on the other half with a more optimized geometry for forward electron transfer. This would increase the ratio of forward to back reaction rates. In the native dimer of *Rb. sphaeroides* we have shown that the hole favours the A half of the dimer. The EPR/ENDOR results, unfortunately, say nothing about the electron that leaves the LUMO. Theoretical calculations have shown that this electron favours the B-half of the dimer.[35] An inspection of the RC structure in *Rb. sphaeroides*[41] reveals that the RC is in the advantageous configuration discussed above, *i.e.*, the B-half of the dimer is closer to B_A, the molecule that is involved in the primary electron transfer step. Thus, the asymmetry is in the right direction to increase the forward to back reaction rates. However, there seems to be an optimum asymmetry. If it is too large, like in the heterodimers, the lifetime of the excited D^+ state is significantly shortened (owing to the large charge-transfer character of the $BChl_A^+$ $BPhe_B^-$ state), which causes a reduction in the quantum yield.[47]

Each of the above arguments can be countered by postulating different structures or ways of accomplishing similar goals. However, it is difficult to come up with an alternative to the dimer that encompasses *all* the above points simultaneously.

One can also speculate on the evolution of the dimer. The two protein subunits L and M of the RC are related to each other by a twofold symmetry axis.[22] Their amino acid sequences are similar,[63] suggesting that they evolved by gene duplication. Perhaps they evolved to accommodate the dimer in a natural way, *i.e.*, one half being associated with the L and the other with the M subunit. There also may have been an additional evolutionary pressure to accommodate the two symmetrically located acceptor quinones Q_A and Q_B that transform electron transfer *via* protonation into a proton gradient.[64]

In conclusion, I hope to have conveyed to you, as promised in the introduction, a feel for the evolution and progress in using EPR/ENDOR to identify and characterize one of the free radicals created in bacterial photosynthesis. The journey has been exciting and we have come much closer to our destination. But we need to keep in mind that we have addressed but one of many problems in bacterial photosynthesis. There are the other reactants: the intermediate, primary, secondary acceptors, and the secondary donor; there is the problem of electron transfers, protonation, *etc.* Much progress has been made in those areas as well and perhaps some of them can be covered in a future Bruker lecture.

Acknowledgements

I am indebted to a large number of students, post-doctoral researchers and collaborators who have contributed to the work described in this talk. The EPR work on D was started with J. McElroy and D. Mauzerall in the late 60s, A. Hoff performed the first ENDOR experiment, E. Lous and M. Huber did the most recent ENDOR/TRIPLE experiments on single crystals. But foremost I would like to thank R. A. Isaacson for his constant and expert help in all the EPR and ENDOR experiments over the past 30 years, to Ed Abresch for providing the seemingly endless supply of purified reaction centres, to C. Schenck for giving us the heterodimer mutant strains, to J. Onuchic and J. Fajer for a helpful discussion, to the Berlin group: W. Lubitz, K. Möbius, F. Lendzian, M. Plato and M. Huber for many stimulating discussions and for their permission to quote some of their unpublished results. The expert advice of M. Y. Okamura as well as many discussions with him are greatly appreciated. The work cited from our laboratory was supported by grants from the National Science Foundation and the National Institutes of Health.

References

1 M. Kamen, *Primary Processes in Photosynthesis*, Academic Press, 1963, p. 4.
2 D. W. Reed and R. K. Clayton, *Biochem. Biophys. Res. Commun.*, 1968, **30**, 471.
3 R. Emerson and W. Arnold, *J. Gen. Physiol.*, 1932, **16**, 191.
4 G. Feher, *Photochem. Photobiol.*, 1970, **14**, 373.
5 R. K. Clayton and R. T. Wang, *Methods Enzymol.*, 1971, **23**, 696.
6 G. Feher and M. Y. Okamura, in *The Photosynthetic Bacteria*, eds. R. K. Clayton and W. Sistrom, Plenum Press, 1978, p. 349.
7 L. N. M. Duysens, Thesis, Univ. Utrecht, 1952.
8 B. Commoner, J. J. Heise and J. Townsend, *Proc. Natl. Acad. Sci. USA*, 1956, **42**, 710.
9 P. Sogo, M. Jost and M. Calvin, *Radiat. Res. Suppl.*, 1959, **1**, 511.
10 J. D. McElroy, G. Feher and D. C. Mauzerall, *Biochim. Biophys. Acta*, 1969, **172**, 180.
11 J. D. McElroy, D. C. Mauzerall and G. Feher, *Biochim. Biophys. Acta*, 1974, **333**, 262.
12 J. D. McElroy, G. Feher and D. C. Mauzerall, *Biochim. Biophys. Acta*, 1972, **267**, 363.
13 G. Feher, A. J. Hoff, R. A. Isaacson and L. C. Ackerson, *Ann. NY Acad. Sci. USA*, 1975, **244**, 239.
14 J. R. Norris, R. A. Uphaus, H. L. Crespi and J. J. Katz, *Proc. Natl. Acad. Sci. USA*, 1971, **68**, 625.
15 G. Feher, A. J. Hoff, R. A. Isaacson and J. D. McElroy, *Biophys. Soc. Abstr.*, 1973, **13**, 61a.
16 J. R. Norris, M. E. Druyan and J. J. Katz, *J. Am. Chem. Soc.*, 1973, **95**, 1680.
17 J. R. Norris, H. Scheer and J. J. Katz, *Ann. NY Acad. Sci.*, 1975, **244**, 260.
18 H. Michel, *J. Mol. Biol.*, 1982, **158**, 567.
19 G. Feher and J. P. Allen, in *Proc. Conf. on Molecular Biology of the Photosynthetic Apparatus*, Cold Spring Harbor Laboratory, New York, 1985, p. 163.
20 J. P. Allen and G. Feher, *Proc. Natl. Acad. Sci. USA*, 1984, **81**, 4795.
21 J. Deisenhofer, O. Epp, K. Miki, R. Huber and H. Michel, *J. Mol. Biol.*, 1984, **180**, 385.
22 H. Michel, O. Epp and J. Deisenhofer, *EMBO J.*, 1986, **5**, 2445.
23 J. P. Allen, G. Feher, T. O. Yeates, D. C. Rees, D. S. Eisenberg, J. Deisenhofer, H. Michel and R. Huber, *Biophys. J.*, 1986, **49**, 583a.
24 C. H. Chang, D. Tiede, J. Tang, U. Smith, J. Norris and M. Schiffer, *FEBS Lett.*, 1986, **205**, 82.
25 J. P. Allen, G. Feher, T. O. Yeates, D. C. Rees, J. Deisenhofer, H. Michel and R. Huber, *Proc. Natl. Acad. Sci. USA*, 1986, **83**, 8589.
26 J. P. Allen, G. Feher, T. O. Yeates, H. Komiya and D. C. Rees, *Proc. Natl. Acad. Sci. USA*, 1986, **84**, 5730.
27 G. Feher, J. P. Allen, M. Y. Okamura and D. C. Rees, *Nature (London)*, 339, 1211.
28 G. Feher, *Phys. Rev.*, 1959, **114**, 1219.
29 C. P. Slichter, *Phys. Rev.*, 1955, **99**, 479.
30 J. E. Wertz and J. R. Bolton, in *Electron Spin Resonance*, McGraw-Hill, 1972, p. 169.
31 J. J. Katz, R. C. Dougherty, H. L. Crespi and H. H. Strain, *J. Am. Chem. Soc.*, 1966, **88**, 2856.

32 W. Lubitz, F. Lendzian, M. Plato, K. Möbius and E. Tränkle, in *Antennas and Reaction Centers of Photosynthetic Bacteria*, Springer, New York, 1985, pp. 164.
33 D. C. Borg, A. Forman and J. Fajer, *J. Am. Chem. Soc.*, 1976, **98**, 6889.
34 F. Lendzian, W. Lubitz, H. Scheer, C. Bukenzer and K. Möbius, *J. Am. Chem. Soc.*, 1981, **103**, 4635.
35 M. Plato, K. Möbius, W. Lubitz, J. P. Allen and G. Feher, in *Perspectives in Photosynthesis*, vol. 22, eds. J. Jortner and B. Pullman, Kluwer Academic Publishers, Dordrecht, 1990, p. 423.
36 G. Feher, *Physica XXIV*, 1958, p. S 80.
37 K.-P. Dinse, R. Biehl, K. Möbius, *J. Chem. Phys.*, 1974, **61**, 4335.
38 K. Möbius, M. Plato and W. Lubitz, *Phys. Rep.*, 1982, **87**, No. 4, 171.
39 R. J. Cook and D. H. Whiffen, *Proc. Phys. Soc.*, 1964, **84**, 845.
40 G. Feher, C. S. Fuller and E. A. Gere, *Phys. Rev.*, 1957, **107**, 1462.
41 J. P. Allen, G. Feher, T. O. Yeates, H. Komiya and D. C. Rees, in *The Photosynthetic Bacterial Reaction Center*, eds. J. Breton and A. Vermeglio, Plenum Press, 1987, p. 5.
42 E. J. Lous, M. Huber, R. A. Isaacson and G. Feher, in *Reaction Centers of Photosynthetic Bacteria*, ed. M. E. Michel-Beyerle, Springer Verlag, Berlin, 1990, p. 45.
43 F. Lendzian, B. Endeward, M. Plato, D. Bumann and W. Lubitz, in *Reaction Centers of Photosynthetic Bacteria*, ed. M. E. Michel Beyerle, Springer Verlag, New York, 1990.
44 F. Lendzian, B. Endeward, M. Plato, K. Möbius, B. Bönigk, W. Lubitz, M. Huber, R. A. Isaacson and G. Feher, to be submitted.
45 T. O. Yeates, H. Komiya, A. Chirino, D. C. Rees, J. P. Allen and G. Feher, *Proc. Natl. Acad. Sci. USA*, 1988, **85**, 7993.
46 M. Huber, E. J. Lous, R. A. Isaacson and G. Feher, *Reaction Centers of Photosynthetic Bacteria*, ed. M. E. Michel Beyerle, Springer Verlag, Berlin, 1990, p. 219.
47 L. M. McDowell, D. Gaul, C. Kirmaier, D. Holten and C. C. Schenck, *Biochemistry*, 1991, **30**, 8315.
48 E. J. Bylina and D. C. Youvan, *Proc. Natl. Acad. Sci. USA*, 1988, **85**, 7226.
49 E. J. Bylina, S. V. Kolaczkowski, J. R. Norris and D. C. Youvan, *Biochemistry*, 1990, **29**, 6203.
50 J. Fajer, D. Brune, M. S. Davis, A. Forman and L. D. Spaulding, *Proc. Natl. Acad. Sci. USA*, 1975, **72**, 4956.
51 M. Huber, R. A. Isaacson, E. C. Abresch, D. Gaul, C. C. Schenck and G. Feher, to be submitted.
52 M. S. Davis, A. Forman, L. K. Hanson, J. P. Thornber and J. Fajer, *J. Phys. Chem.*, 1979, **83**, 3325.
53 W. Lubitz, R. A. Isaacson, E. C. Abresch and G. Feher, *Proc. Natl. Acad. Sci. USA*, 1984, **81**, 7792.
54 P. J. O'Malley and G. T. Babcock, *Proc. Natl. Acad. Sci. USA*, 1984, **81**, 1098.
55 A. De Groot, A. J. Hoff, R. De Beer and H. Scheer, *Chem. Phys. Lett.*, 1985, **113**, 286.
56 C. P. Lin and J. R. Norris, *FEBS*, 1986, **197**, 281.
57 F. Lendzian and W. Lubitz, personal communication.
58 F. Lendzian, K. Möbius, M. Plato, U. H. Smith, M. C. Thurnauer and W. Lubitz, *Chem. Phys. Lett.*, 1984, **111**, 583.
59 M. Plato, K. Möbius and W. Lubitz, in *Chlorophylls*, ed. H. Scheer, CRC Press, Boca Raton, Florida, 1991, ch. 410, p. 1015.
60 M. Plato, personal communication.
61 I. M. Olson and R. K. Clayton, *Photochem. Photobiol.*, 1966, **5**, 655.
62 R. A. Marcus and N. Sutin, *Biochim. Biophys. Acta*, 1985, **811**, 265.
63 H. Komiya, T. O. Yeates, D. C. Rees, J. P. Allen and G. Feher, *Proc. Natl. Acad. Sci. USA*, 1988, **85**, 9012.
64 M. Y. Okamura and G. Feher, *Ann. Rev. of Biochem.*, 1992, **61**, 861.

Paper 2/02500K
Received 14*th May* 1992
Accepted 28*th May* 1992